International Journal of Electronics and Applied Research (IJEAR) **2014, 1, 1-14**
Published Online June 2014 (*http://eses.co.in/ESES Journal)* ISSN NO: 2395-0064

Dynamics of Driven Colpitts Oscillator in Presence of Co-channel Tone Interference: An Experimental Study

Suvra Sarkar[1*], Sandeepa Sarkar[2#], B C Sarkar[3$]

[1]*Electronics Department, Burdwan Raj College, Burdwan 713104, WB*

[2]*Burdwan Harisabha Hindu Girls High School (Morning), Burdwan-713104, WB*

[3]*Physics Department, Burdwan University, Burdwan-713104, WB*

* *suvrabrc@gmail.com*

[#]*sandeepaphys@gmail.com*

[$]*bcsarkar_phy@yahoo.co.in*

Abstract

In the present paper, the dynamics of a conventional BJT based Colpitts Oscillator (CO) in presence of a driving signal along with a co-channel tone interference signal is thoroughly examined. We perform an experiment in the radio frequency range with a proto type hardware circuit. The same experiment is repeated by simulation using a circuit simulator. Broad band continuous spectra is observed both in the upper and the lower side of the synchronization band of the CO just 'out of lock' condition. This indicates a chaotic mode of oscillation of the CO in the driven condition. By suitably adjusting the strength and the frequency of the interference signal, a broadening in the bandwidth of the chaotic spectra is observed. We also study the system dynamics numerically using ac equivalent model of the CO. Numerical simulation results are found to be in agreement with the experimental observations. The study reveals that a periodic CO, forced by two close frequency sinusoidal signals, can be used to generate chaotic signal in a controllable manner. The proposed method of chaos generation has application potential in chaos based electronic communications.

Key words: BJT; Colpitts Oscillator; Co-channel Tone Interference.

1. Introduction

In the last few decade researchers have paid considerable attention in studying the nonlinear dynamics of different electronic circuits and systems [Alligood et al., 1996 ; Hilborn, 2000]. For many years, electronic oscillators generating periodic signals find applications in communication system to design amplifiers, oscillators, modulators/demodulators or electronically controllable phase shifters etc. However, as an oscillator circuit has inherent nonlinearity then by suitably adjusting system parameters its operating regimes can be expanded to observe some interesting features like bifurcations, chaos, intermittency, crisis etc. A chaotic signal which is apparently random and noisy finds applications in different secure communication systems. This is because chaotic signals have broad frequency band that can withstand the problem of multi path and frequency selective fading. Chaos can also be used for mapping of information bits. Due to these reasons studies on the chaotic dynamics of different nonlinear circuits have attracting the researchers [Stogartz, 1994 ; Alligood et al., 1996 ; Hilborn, 2000 ; Kennedy et al., 2000]. Several algorithms for generating chaotic signals in deterministic way have been reported in the literature [Kennedy, 1994 ; Chakravorty et al., 2009 ; Sarkar, 2012 ; Li et al., 2013]. Among different types of RF and microwave oscillators used as chaos generators, application of Colpitts Oscillator (CO) is well known. This is because of its circuit simplicity, lesser power requirement, high operating frequency limit etc. Available literature indicates different techniques like variation of circuit design parameter or operating bias current or resonant perturbation by harmonic signal are often used to make CO to operate into chaotic mode [Qiao et al., 2007 ; Sarkar et al., 2013 ; Sarkar et al., (in Press)]. But, to the knowledge of the author, studies on the effect of two forcing signal of adjacent frequency on the dynamics of periodic CO remains unexplored. In the present paper interest has been given on this problem. We have thoroughly examined the CO dynamics driven simultaneously by two forcing signals, one as synchronizing signal and the other as interfering signal. For this purpose, experiment using a prototype circuit is done in radio frequency range with the help of circuit simulator and then by hardware arrangement. We have observed, depending on frequency and strength of the injecting signals, CO dynamics show a number of complex behavior. This is because of nonlinear interaction of the active device of the oscillator with the external adjacent frequency signals. We have also included results of numerical investigations based on the system equations of the oscillator.

The paper is organized in the following way. In section 2, experimental study on the performance of forced oscillator system, first by using a circuit simulator and then by performing actual hardware experiment is reported. In section 3, we formulate system equations using the ac equivalent circuit of

the BJT based CO considering the effect of bias current. Results of numerical simulations are presented in section 4. Finally, some concluding remarks are included in section 5.

2. Experimental Studies

The functional block diagram of the experimental arrangement is shown in Figure 1. To perform the experiment a bias current controlled CO circuit as shown in Figure 2(a) is arranged. Here, the basic oscillator is designed using a 2N2222A type transistor (Q) (having transition frequency 300MHz) and some passive components like an inductor (L), capacitors (C_1, C_2 and C_0), resistors R_1, R_2. Its dc bias current is adjusted by using the current mirror circuit [Sarkar et al ., 2013] which is designed using a pair of

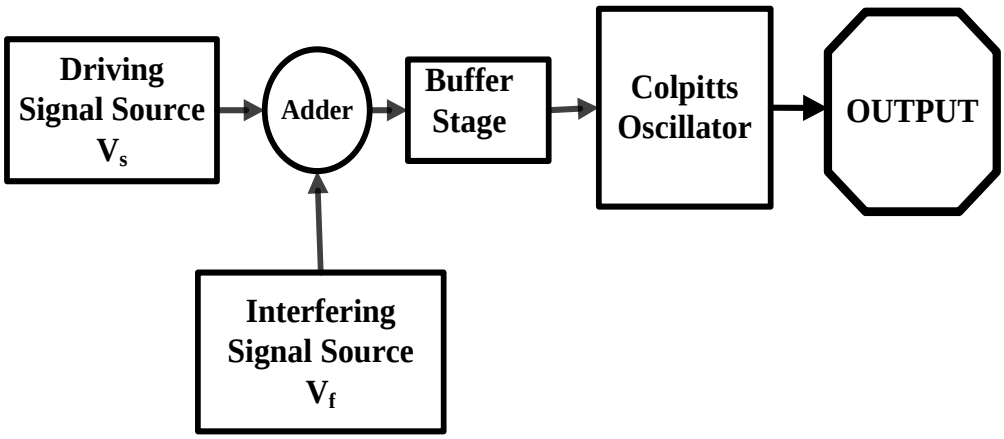

Figure 1. Functional block diagram of the driven Colpitts oscillator in presence of interfering signal

identical transistors and a variable resistor R_X. By varying R_X, the bias current is adjusted properly so that the CO can operate in period-1 state in free running condition. External forcing signal taken from a signal generator is applied at the emitter terminal. We perform both the simulation experiment (using circuit simulator) and hardware experiment on the circuit. Here we choose the bias current of the CO as 4.0mA to get period-1 oscillation in free running state. In this condition the frequency and peak output amplitude of the CO is obtained as 151 kHz and 1.4 volts respectively. Figure 3(a) shows the output spectral characteristics and the phase plane plot (inset) of the oscillator in free running condition as obtained using circuit simulator. The voltages at the collector terminal and the emitter terminal are chosen as the state variables to plot the phase-plane diagram. Corresponding observations of the hardware experiment is presented in Figure 3(b).

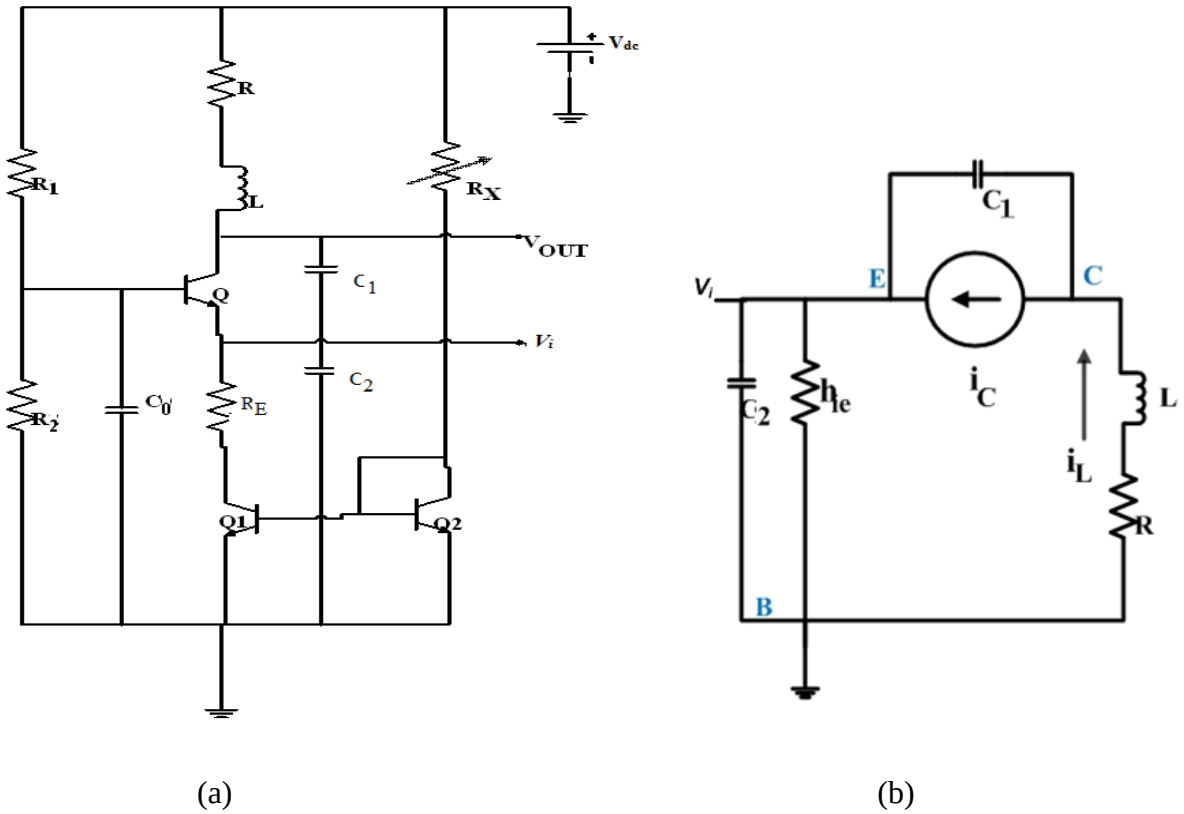

Figure 2. (a) Circuit diagram of the bias current controlled driven Colpitts Oscillator in presence of interfering signal (V_i= V_s+V_f , The values of circuit components : R_1=R_2= 2.2KΩ, R=10Ω, R_E=10Ω, C_0=1μF, L=0.055mH, C_1=C_2= 0.1μF, R_x= 10kΩ variable resistor, Q, Q1 and Q2 are 2N2222A NPN transistors; DC supply voltage V_{dc} = 5.2 volts.). (b) ac equivalent circuit of the driven Colpitts oscillator with a voltage-dependent current source model for the transistor.

To study the effect of the interfering signal on the dynamics of the driven CO, at first we examine its dynamics in presence of a driving signal taking from a signal generator. Keeping strength of the driving signal fixed at 0.14 volts (i.e. 10% of the strength of the free running CO), its frequency is gradually varied from low to a high value, such that the driven oscillator passes through asynchronous mode and then enters into synchronized state. The bandwidth of synchronization is observed 23 kHz. Crossing this state, it again enters into asynchronous 'out of lock' state at higher frequency side. During this process, the CO dynamics is critically examined. This study is repeated for different strength of the driving signal. It has been observed synchronization band (SB) of the CO increases with the increases of the strength of the driving signal. This is shown in Figure 4. By adjusting strength and frequency of the driving signal broad band continuous spectrum is observed at 'out of lock' condition both at the upper and the lower side of the SB of the driven CO. Figure 5 and Figure 6 show some of the observed output spectra with the variation of the frequency of driving signal. Figure 5.

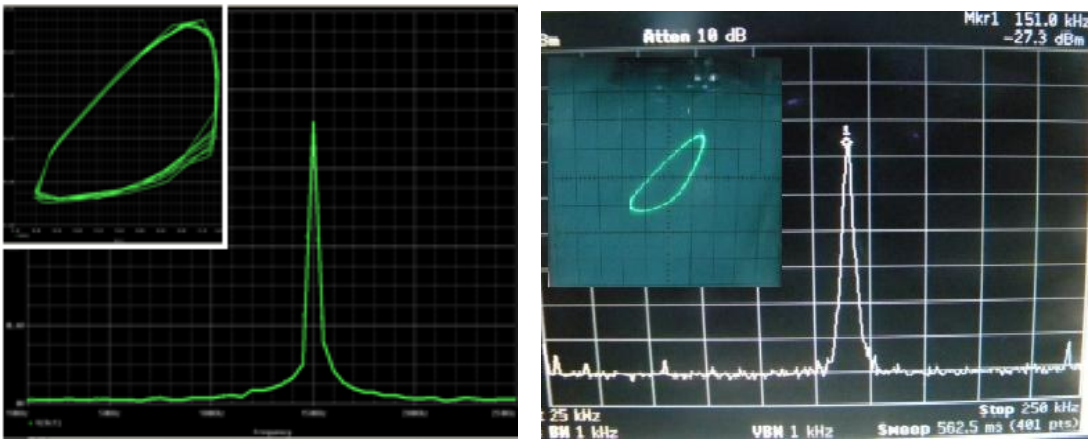

(a) (b)

Figure 3. Experimentally obtained output spectra and phase plane plot (inset) of the free running CO (a) using circuit simulator, (b) from hardware circuit.

represents results as obtained using circuit simulator and Figure 6 gives corresponding hardware experimental results. In this context, we mention that bias current of the free running CO plays an important role in the synchronization properties of the driven CO. It has been observed, if the bias current of the free running CO crosses a certain limit, although it oscillates in Period-1 state, but instead of showing synchronization behavior with the driving signal it shows different complex behavior. Keeping the strength of the driving signal fixed at about 10% of the free running amplitude of the oscillator, it has been observed that SB of the CO decreases with the increase of the bias current. Then keeping the bias current at some higher value, we critically examine the CO dynamics by slowly changing the driving signal frequency from low to high value around the fundamental frequency of the CO. Transition from period-1 to chaotic state of oscillation through period doubling route is observed[Sarkar et al., 2014].

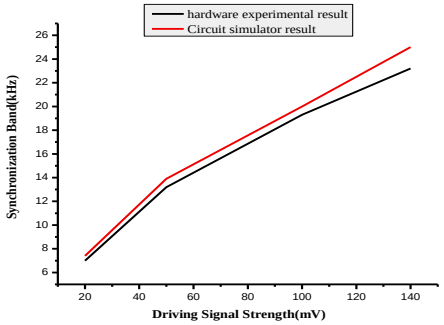

Figure 4: Variation of synchronization band of the CO with the strength of the driving signal

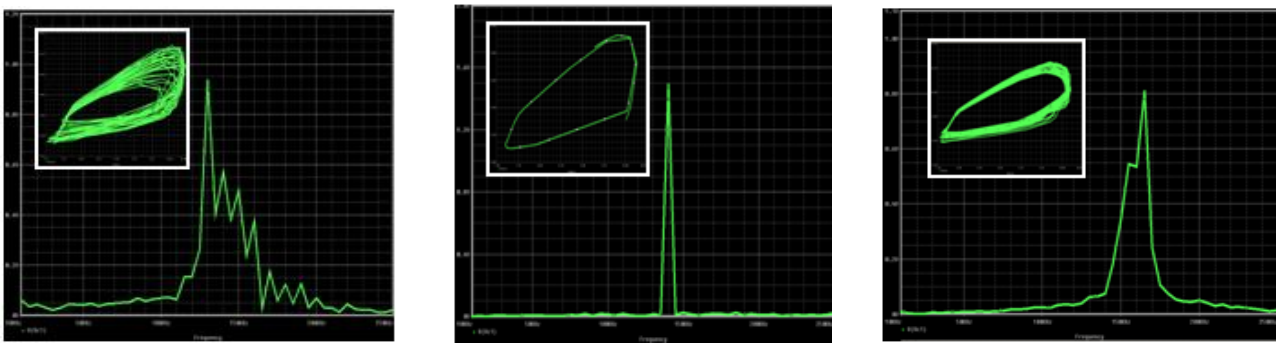

(a) (b) (c)

Figure 5.Experimentally (using circuit simulator) obtained output spectra and phase plane plot (inset) of the driven CO without interfering signal , v_s=140 *mv*) (a) f_s=134.3KHz , (b) f_s=144KHz , (c) f_s=167.7KHz.

In the next part of the experiment, we have applied the interfering signal (having strength0.06 v*olts* i.e. about 43% of the driving signal strength) along with the synchronizing signal. It is taken from another signal generator.

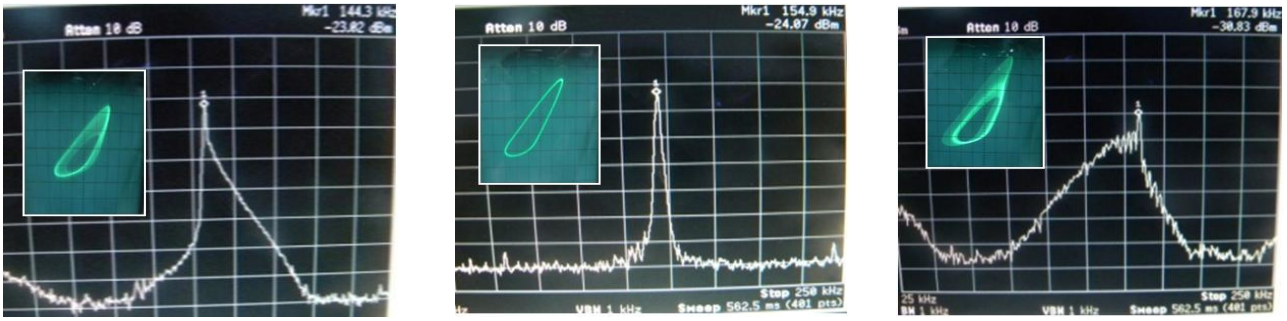

(b) (c)

Figure 6. Experimentally (from hardware experiment) obtained output spectra and phase plane plot (inset) of the driven CO for different frequency of the driving signal without interfering signal (v_s=140 mV) (a) f_s=144.3KHz (b) f_s=155KHz , (c) f_s=167.9KHz.

The two forcing signals are added with the help of an adder circuit designed using operational amplifier and then the resultant signal is applied to the emitter terminal of the CO through a suitable buffer circuit (designed using operational amplifiers). In this condition, keeping frequency of the interfering signal fixed (at 138 k*Hz* ie at the lower side of the lock band but out of lock condition) frequency of the synchronizing signal is varied gradually from low to high value crossing the SB of the CO. Corresponding output spectra are examined. It has been observed, for some specific frequency detuning, broad band continuous spectrum having band width larger than the interference

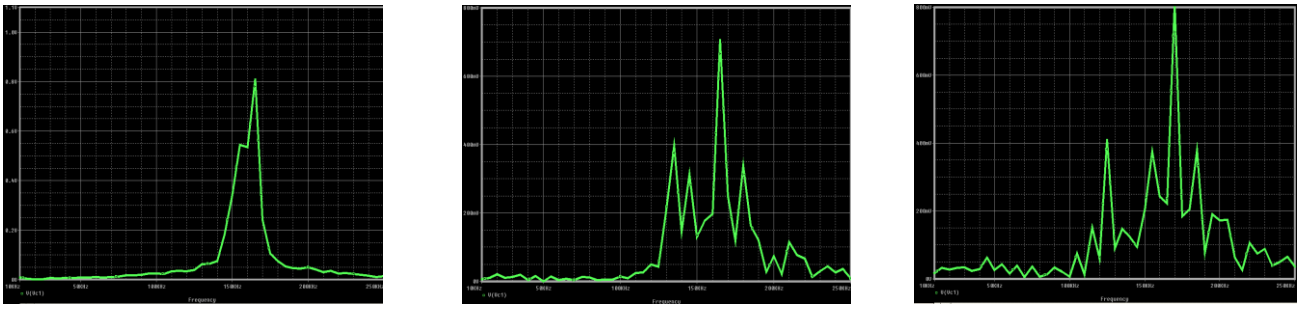

(a) (b) (c)

Figure 7. Experimentally obtained (using circuit simulator) output spectra of the driven CO for different strength of the interfering signal(V_s= 140*mv*, f_f = 138 *kHz*) (a)V_f= 0 *volst*, f_s= *168kHz* , (b) V_f= 60*mv*, f_s =161kHz (c) V_f=80*mv*, f_s =155kHz

free condition is observed both at the upper side and the lower side of the lock band. The results of the circuit simulator and those obtained from hardware experiment are given in Figure 7 and Figure 8 respectively. As strength of the interfering signal is increased, enhancement in the bandwidth of the broad band spectra is observed. Table: I presents the measured -30dB bandwidth of the output spectra for different strength of the interfering signal.

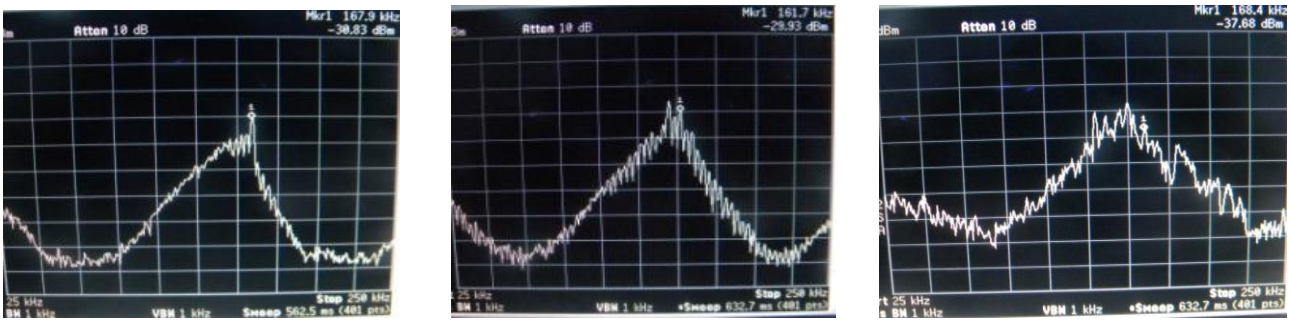

(a) (b) (c)

Figure 8. Experimentally obtained output spectra of the driven CO for different strength of the interfering signal(V_s= 140*mv*, f_f = 138 *kHz*) (from hardware experiment) (a)V_f= 0 *volts*, f_s= *167kHz* , (b) V_f= 60*mv*, f_s = 161kHz (c) V_f=80*mv*, f_s = 155kHz

3. Mathematical Model of the Driven Colpitts Oscillator in presence of Co-channel Interference signal

To analyze numerically the dynamics of the oscillator under study, the hardware circuit is replaced by its ac equivalent model as shown in Figure 2 (b). Here, the effect of variation of bias current in the

free running CO is taken into consideration. We replace the active device (the BJT operating in the common base mode) by a nonlinear voltage controlled current source that delivers the collector current i_c [Sarkar et al. ,2013]. It is a function of the voltage across the base and the emitter terminals of the device (v_{be}), written as,

$$i_c = f(v_{be}) \tag{1(a)}$$

$$\text{Where, } f(v_{be}) = g_{m1}v_{be} - g_{m3}v_{be}^3 \tag{1(b)}$$

g_{m1} and g_{m3} are the parameters representing linear and nonlinear trans-conductance of the device. We normalize g_{m1} and g_{m3} in terms of the linear trans-conductance g_{m10} of the transistor at the quiescent current I_o required for periodic operation of the CO. We write g_{m1} and g_{m3} as ag_{m10} and bg_{m10} respectively, where a and b are the parameters taking care of the actual operating bias current. Intuitively the magnitude of b is much less than that of a, since the response is linear for small values of v_{be}. The effects of junction capacitance are not explicitly considered here, because, their magnitudes are very small and hence their reactances are very high at the frequency of operation of the CO. Effect of the synchronizing signal and the interfering signal is considered by adding an additional voltage source (v_i, which is combination of these two signal) to the emitter terminal of the equivalent circuit.

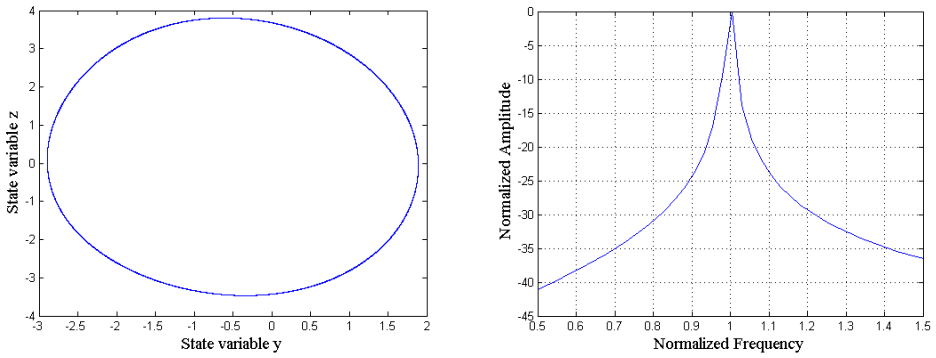

Figure 9: Numerically computed phase plane (y-z) plot and frequency spectrum of the free running CO. system parameters are: a=1.9, g=1.32, Q=4.0, k=0.5, h_r=0.04, b=0.2.

Then, using basic circuit theoretic laws, we obtain the following set of differential equations describing the system dynamics:

$$\frac{dv_{c1}}{dt} = -\frac{(i_L + f(-v_{c2} + v_i))}{C_1} \tag{2(a)}$$

$$\frac{dv_{c2}}{dt} = -\frac{i_L}{C_2} - \frac{v_{c2}}{h_{ie}C_2} + \frac{v_i}{C_2} \tag{2(b)}$$

$$\frac{di_L}{dt} = \frac{(v_{c1} + v_{c2} + v_i)}{L} - \frac{Ri_L}{L} \qquad 2(c)$$

Here v_{C1} and v_{C2} are the voltages across C_1 and C_2 respectively and i_L is the load current. v_i, the injected voltage is sum of the synchronizing voltage (v_s) and the co channel interfering voltage (v_f). We consider

$$v_s = V_s \sin(\omega_s t) \qquad 3(a)$$

$$v_f = V_f \sin(\omega_f t + \theta) \qquad 3(b)$$

Here, V_s and $\omega_s = (2\pi f_s)$ represent the strength and the angular frequency of the synchronizing signal. V_f and $\omega_f (= 2\pi f_f)$ are the corresponding values of the interfering signal. θ is the phase constant. We normalize voltage variables by v_T (temperature equivalent of voltage i.e.) kT/q [Sedra and Smith, 2004] and the current variable by I_0, (mentioned earlier) to get dimensionless state variables x, y and z. In terms of these variables, the state equations can be obtained in the dimensionless form as follows:

$$\frac{dx}{d\tau} = \frac{g(-z + a(y + v_{sn} + v_{fn}) - b(y + v_{sn} + v_{fn})^3)}{Q(1-k)} \qquad 3(a)$$

$$\frac{dy}{d\tau} = \frac{-gz - h_r y - g(v_{sn} + v_{fn}))}{Qk} \qquad 3(b)$$

$$\frac{dz}{d\tau} = \frac{Qk(1-k)((x+y) + v_{sn} + v_{fn})}{g} - \frac{z}{Q} \qquad 3(c)$$

We have substituted $\tau = \omega_0 t$, $\omega_0^{-1} = \sqrt{LC_1C_2/(C_1 + C_2)}$, $x = v_{c1}/v_T$, $y = v_{c2}/v_T$, $z = i_L/I_0$, $h_r = L/(R(C_1 + C_2)h_{ie})$, $g = LI_0/(R(C_1 + C_2)v_T)$, $Q = \omega_0 L/R$, $k = C_2/(C_1 + C_2)$, $v_{sn} = V_{sn}\sin(\omega_{sn}\tau)$, $v_{fn} = V_{fn}\sin(\omega_{fn}\tau + \theta)$, $V_{sn} = V_s/v_T$, $V_{fn} = V_f/v_T$, $\omega_{sn} = \omega_s/\omega_0$, $\omega_{fn} = \omega_f/\omega_0$,. The parameters g, ω_0 and Q are the amplifier gain, resonant frequency and the quality factor of the resonant circuit respectively.

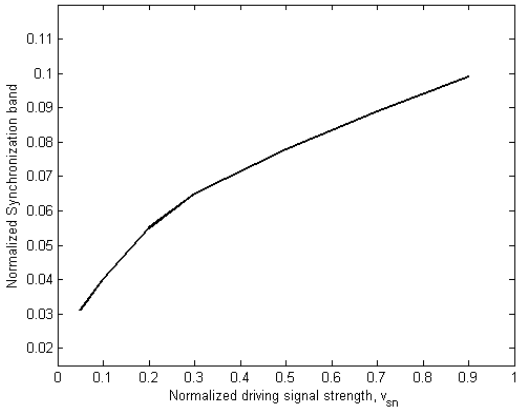

Figure 10. Numerically computed synchronization band of the Colpitts oscillator for different strength of the driving signal. The system parameters are: a=1.9, g=1.32, Q=4.0, k=0.5, h_r=0.04, b=0.2.

4. Numerical Simulation of the system under study

To understand the dynamics of the driven CO in presence of co channel tone interference, system equations as presented in (3) are numerically solved for a judiciously chosen set of system parameters. Here, we have taken 4th order Runge-Kutta integration algorithm in the normalized time domain with a step size h=0.01. To exclude initial transients in the numerical solution and to get steady state values of the state variables, we have discarded more than 50% of the data points close to initial time. The values of the parameters k, g, Q and h_r of CO under study have been taken in accordance with the designed hardware circuit (described in Section 2). They are taken as g = 1.32, Q = 4.0, k = 0.5, h_r = 0.04, b = 0.2.

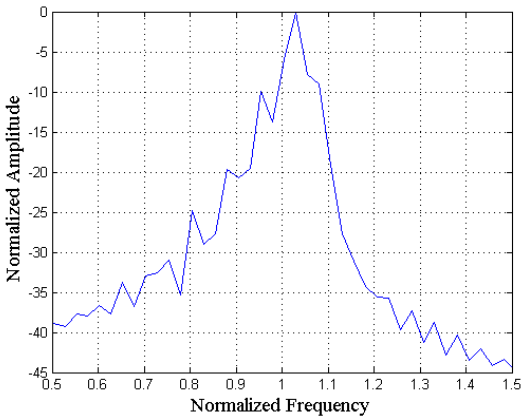

(a)

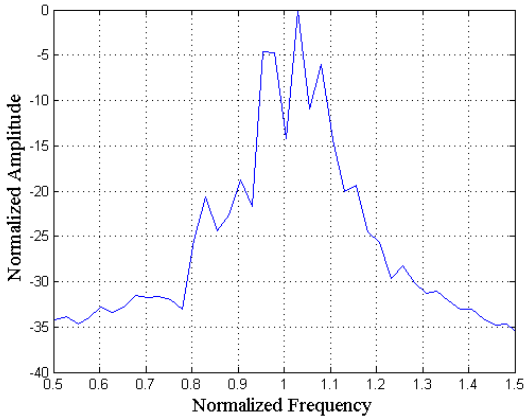

(b)

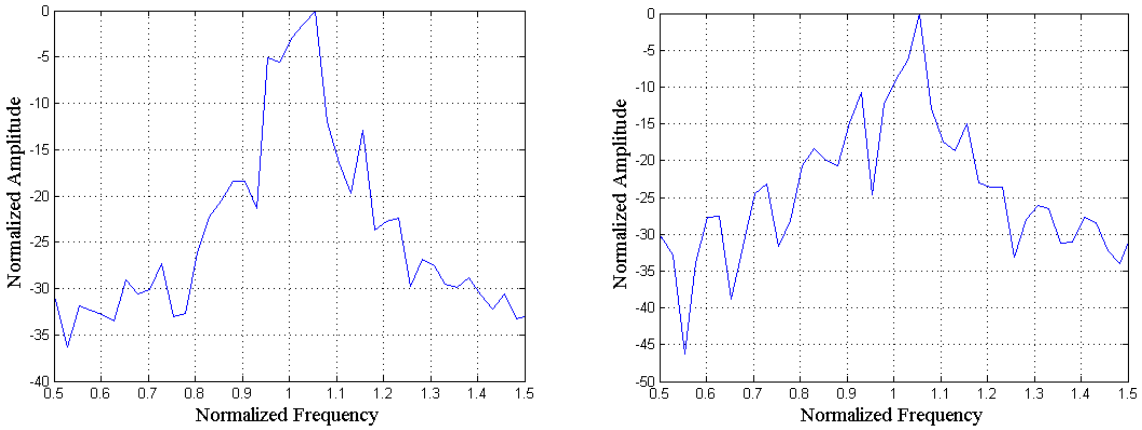

(c) (d)

Figure 11. Numerically computed output spectra of the driven CO for different strength of the interfering signal (The system parameters are: a=1.9, g=1.32, Q=4.0, k=0.5, h_r=0.04, b=0.2, V_{sn}=0.4, ω_{fn} =0.95, ω_{sn} =1.063)(a) V_{fn}=0, (b) V_{fn}=0.16, (c) V_{fn}=0.20, (d) V_{fn}=0.22

The state variable z represents the instantaneous value of the oscillator output in the time domain. The value of parameters a and b in (3) are taken in the periodic region of operation for the CO (a=1.9, b=0.2). Figure 9(a) and Figure 9 (b) show respectively the numerically obtained phase plane plot (y-z) and the frequency spectrum of the free running CO. Then, we consider the effect of the driving signal v_{sn} on the CO dynamics. Keeping the value of V_{sn} fixed at 0.4 (about 10% of the free running amplitude of the CO), ω_{sn} is varied gradually around the normalized frequency of the free running CO. To study the system response, state space trajectory (in the y-z plane) and the frequency components present in the oscillator output (obtained by first Fourier transform (FFT) of time samples of z) is examined. It is observed for a certain range of ω_{sn} , CO is in synchronized state with the driving signal. In this situation, the frequency of the CO becomes same as that of the external driving signal even though it is different from the free running frequency of the CO. Fig 10 shows the nature of variation of SB with the variation of driving signal strength. Both in the upper and the lower side of the SB, broad band continuous spectrum although asymmetric in nature are observed. It indicates possibility of chaotic oscillation in the CO dynamics. In the next stage, effect of v_{fn} along with v_{sn} is considered. Keeping the value of V_{sf} and ω_{sf} fixed (V_{sf} =0.16 and ω_{sf} =0.95), ω_{sn} is gradually varied. It is observed for some specific value of ω_{sn} (both in the upper side and the lower side of the lock band), spectral broadening in the bandwidth of the chaotic signal compared to interference free condition occurs. Some of the obtained results are given in Fig 11. It indicates bandwidth of the continuous spectra increases as the strength of the interfering signal increases;

Table II represents an estimation of- 30dB bandwidth of the chaotic spectra as obtained from simulation studies for different strength of the interfering signal.

Table I

Experimentally obtained (from hardware experiment) -30 dB bandwidth of the chaotic spectra for different strength of the interfering signal **(**f_f=138 KHz, f_s= 167 kHz, V_s=0.14V**)**

V_f in mv	-30 dBm bandwidth at the upper side of the SB
0	50KHz
60	56.25 KHz
80	65 KHz
100	77 kHz

Table II

Numerically obtained -30 dB bandwidth of the chaotic spectra for different strength of the interfering signal **(**ω_{fn} =0.95, V_{sn}=0.4, ω_{sn} = 1.065*)*

V_{fn}	-30 dBm bandwidth(normalized) at the upper side of the SB
0	0.35
0.16	0.50
0.20	0.60
0.22	0.70

5. Conclusion

The dynamics of a driven CO in presence of co-channel interfering signal is extensively studied experimentally using circuit simulator, through hardware circuit and also by numerical simulation. This study confirms occurrence of synchronization behavior of the driven CO for a proper set of system and driving signal parameters .Besides this, the present study reveals that CO can generate chaotic oscillations (as its output shows broad band continuous spectrum) both in the lower and the

upper side of its synchronization band, in 'out of lock' condition. In presence of interfering signal of suitable strength and frequency, broadening in the bandwidth of the continuous spectra is possible. Observations of both the hardware experiment and that obtained from the circuit simulator are consistent with the results of the simulation experiment. Therefore, a CO driven by synchronizing signal along with an interfering signal can be used to generate broad band chaotic signal in controllable manner. In this direction the study reported in this paper has practical importance along with an academic interest.

Acknowledgement

Authors acknowledge the infrastructural support received in Physics department, Burdwan University through sponsored research project from the DST (India) and in the PURSE program sponsored by the DST.

References

Alligood K. T., Sauer T. D., Yorke J. A. Chaos: An Introduction to Dynamical Systems. *Published by Springer*, 1996.

Chakravorty J. et al. Generating chaos in injection-synchronized Gunn Oscillator: An experimental approach. *IETE Journal of Research*. **55**, 106-111, 2009.

Hilborn R. C. Chaos and Nonlinear dynamics *Oxford University Press*, 2000.

Kennedy M. P., Rovatti R., Setti G. Chaotic Electronics in Telecommunications. Published by *Taylor and Francis*, 2000.

Kennedy M. P. Chaos in the Colpitts oscillator. *IEEE Trans on Circuits and Systems I: Fundamental Theory and Applications*. **41**, 11, 771-774, 1994.

Li J. X., Wang Y. C, Chang F. M. Experimental demonstration of 1.5 GHz chaos generation using an improved Colpitts oscillator. *Nonlinear Dynamics*, 2013.

Qiao S. et al. A new architecture of UWB radar utilizing microwave chaotic signals and chaos synchronization. *Progress in Electromagnetic Research.* **75**, 225-237, 2007.

Sarkar B. C et al. Some numerical and experimental observations on the growth of oscillations in an X-band Gunn oscillator. *Progress in Electromagnetics Research B*. **40**, 325-341, 2012.

Sarkar S., Sarkar S., Sarkar B. C. On the Dynamics of a Periodic Colpitts Oscillator Forced by Periodic and Chaotic Signals, *accepted for publication in Communications in Nonlinear Science and Numerical Simulations*. Elsevier. (in press)

Sarkar S., Sarkar S., Sarkar B. C. Nonlinear dynamics of a BJT based Colpitts oscillator with tunable bias current. *International Journal of Engineering and Advanced Technology*, **2**, 12-18, 2013.

Sarkar S., Sarkar S., Sarkar B. C. Effect of Bias Current on the Synchronization Characteristics of Colpitts Oscillator, *in proceedings of the National Conference on Materials, Devices and Circuits in Communication Technology, MDCCT 2014*,7– 8 February, 2014.

Sedra A. S. and Smith. K. C. Microelectronic Circuits. *Oxford University Press*, 2004.

Stogartz S. H. Nonlinear dynamics and Chaos: with Applications to Physics, Biology, Chemistry and Engineering. *Addison Wesley Publishing*, 1994.

